Warwick iGEM 2019

Biochemical COPASI Enzyme Simulation of Fatberg Degradation

Design

Michaelis–Menten Kinetics and the *In Vitro* Model

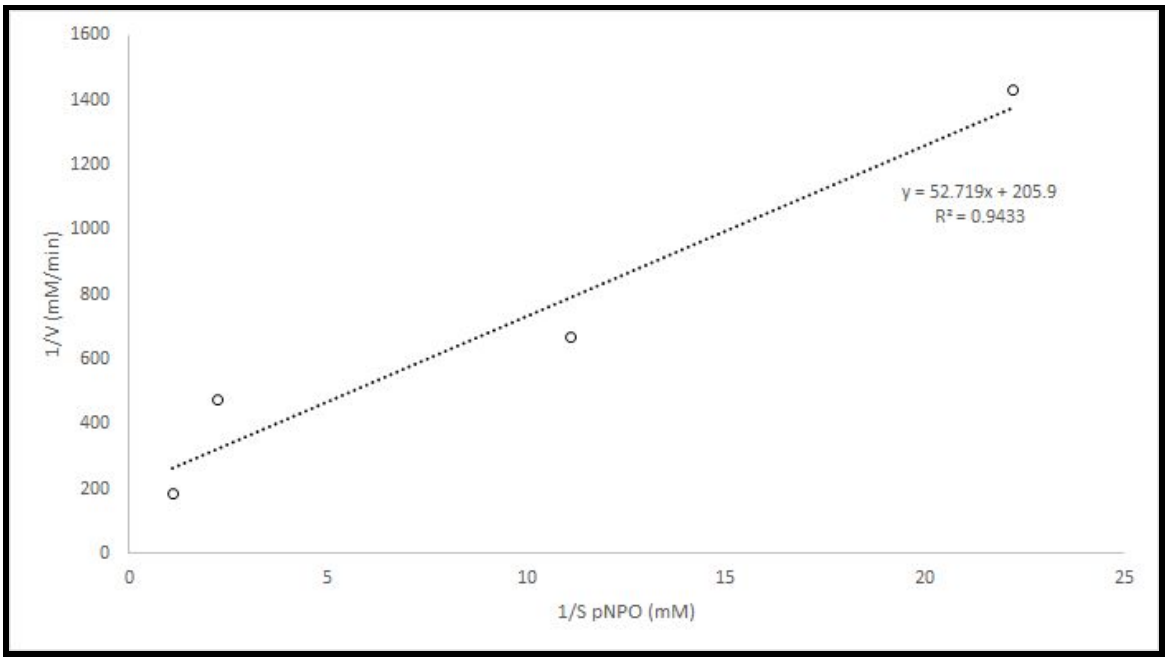

Figure 1. TliA Kinetics Characterisation via Lineweaver-Burk Plot. Thermostable lipase A (TilA - BBa_K258006) has a *KM of 0.256mM* and a *Vmax of 0.00375 mM/min*, where the *Kcat is 0.0972 mM / min / mg*.

Pseudomonas fluorescens (SIK W1) Thermostable lipase (TliA) activity was determined by change in light absorbance at a wavelength of 400nm, which directly correlated to the concentration of p-Nitrophenol (pNP), caused by lipolysis of p-Nitrophenol octanoate (pNOP) substrate. The data defining enzyme activity was processed into kinetic data for TliA.

Once the Kinetic characterisation of the enzyme had been determined from **Figure 1**, the data could be processed into a biochemical simulation using the program COPASI. (copasi.org)

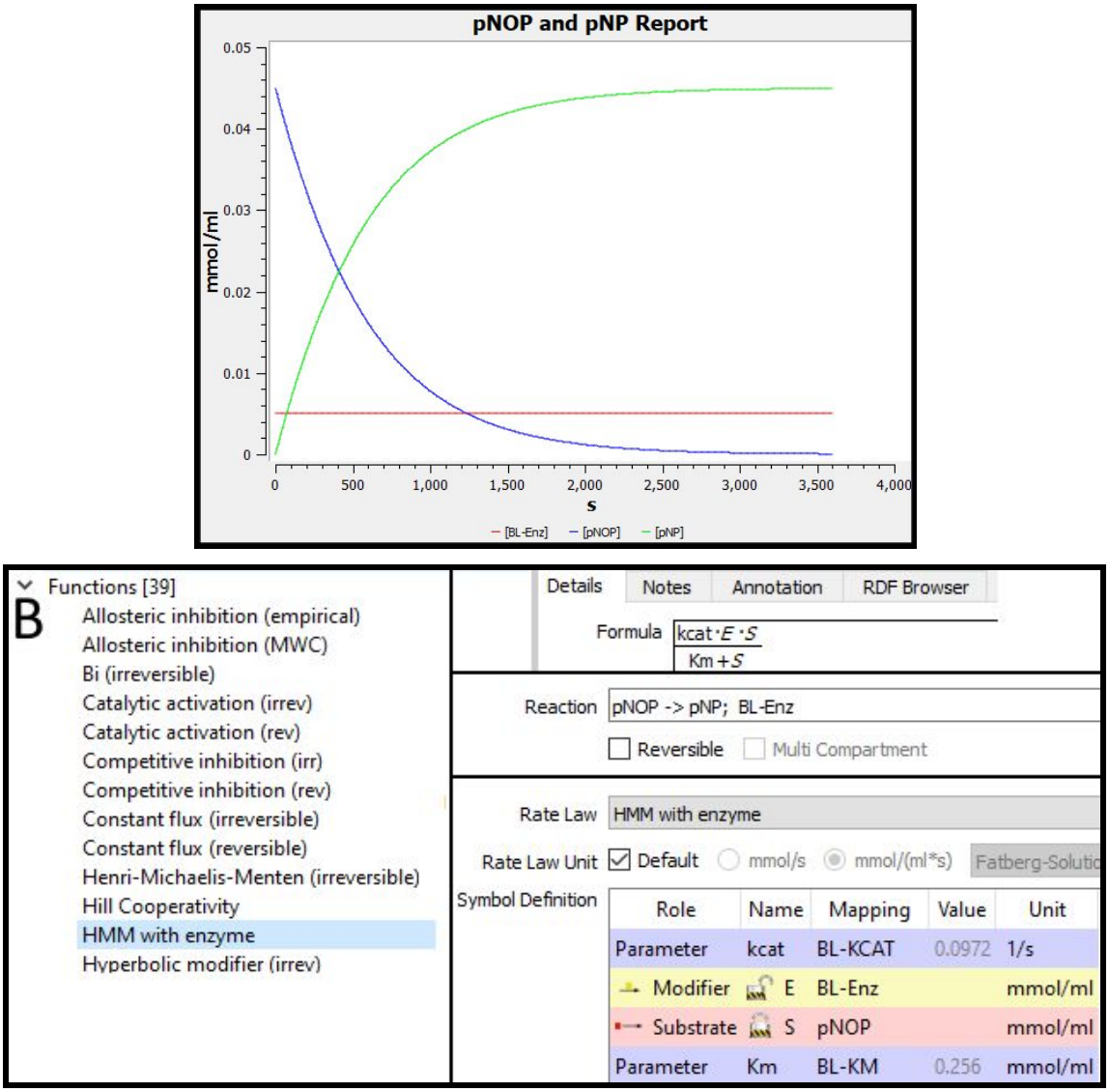

Figure 2. HMM with Enzyme Formula. A. An early simulation of the TliA lipase enzyme within a p-Nitrophenol octanoate assay. **B.** The Henri-Michaelis-Menten law with an Enzyme has previously been defined in COPASI. The process was appropriately adapted from page 10 of a tutorial regarding the model of MAPK proteins in COPASI: (https://2019.igem.org/File:T--Warwick--2019-MichMentenCOPASI-Archive.pdf)

An initial model was designed to replicate the characterisation experiment shown in **Figure 1**. The Km of 0.256 mM and Kcat of 0.0972 mM / min / mg, which were derived from experimental data collected through p-Nitrophenol octanoate assays in the laboratory, can be applied to the Lipase enzyme (BL-Enz) **Figure 2B**. The values derived from the real assay can then be used to simulate an assay on COPASI, which can then be compared to the actual data. **Figure 2A.**

Developing *In Vivo* Model

A simple *in vitro* model was composed in **Figure 2A** and demonstrated a realistic trend. A more intricate *in vivo* model can be constructed using the *in vitro* model as a template by combining the data gathered in the lab with data presented in publications.

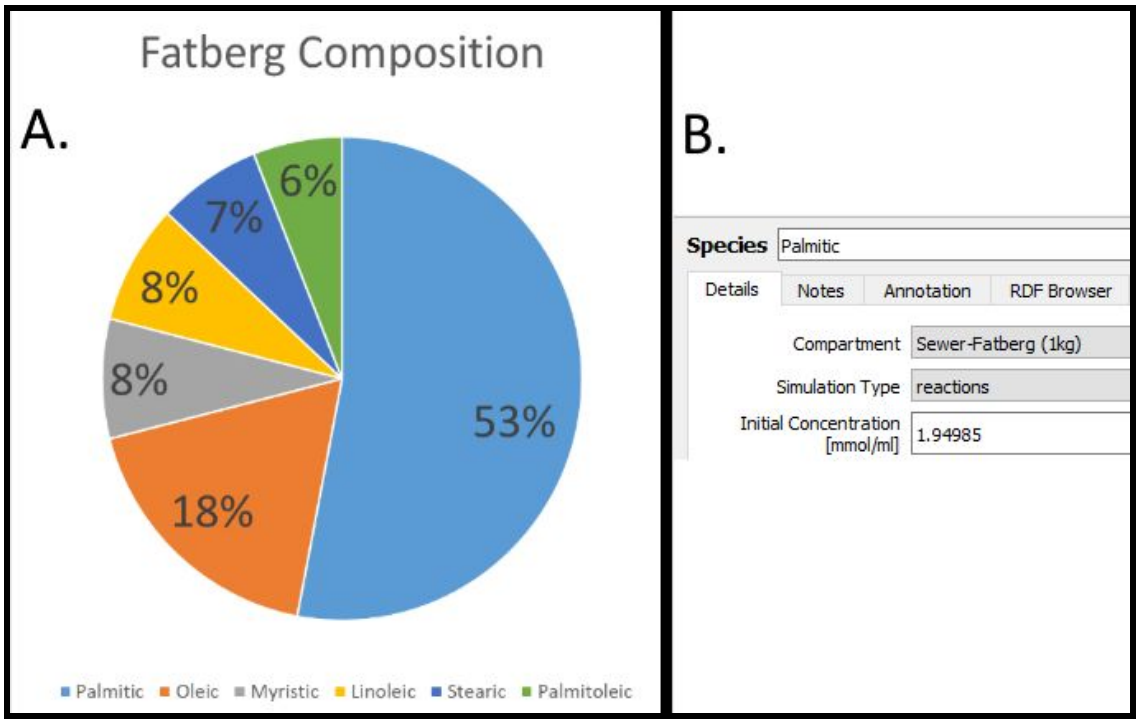

Figure 3. Fatberg Composition. Fatbergs are comprised of a range of fats - different fatty acid tail lengths can alter the degradation and solubility properties of fats within the fatberg. **(Fatty Chain, Composition percentage)**: (Palmitic, 53%); (Oleic, 18%); (Myristic, 8%); (Linoleic, 8%); (Stearic, 7%); (Palmitoleic, 6%). The data has been adapted from a document on Fatberg Analysis by the Museum of London, Figure 1B. **(**https://2019.igem.org/File:T--Warwick--2019-Fatberg-Report-Archive.pdf)

The *in vivo* model has been designed to simulate the digestion of one kilogram of fatberg. The data in **Figure 3** was used to calculate the initial concentrations regarding the variety of fats in the fatbergs. Fatbergs are mostly fats, wherein the varying fatty chains constitute a different percentage of the composition (**Figure 3A**).

A unique initial concentration was determined for each fatty chain. For example, palmitic chains composed 50% of the fatberg and as such made up 500g of fat per litre, then the mass of palmitic fats was divided by their fatty acid molecular mass in order to convert from grams per litre to mmol/ml, resulting in an initial concentration of 1.94985 mmol/ml (**Figure 3B**).

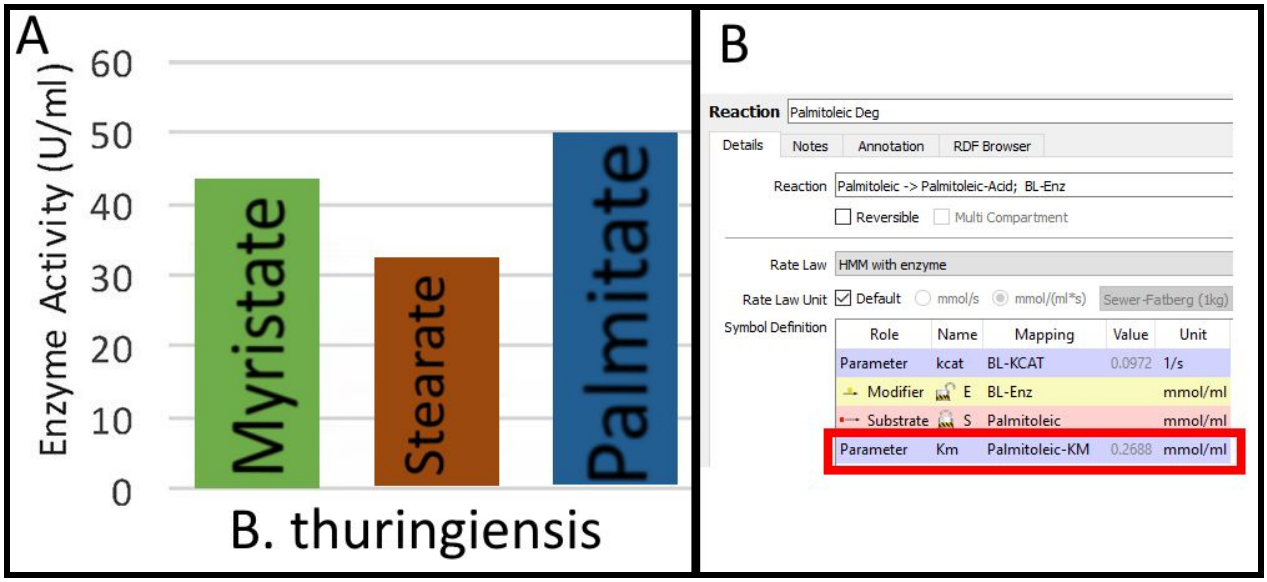

Figure 4. Enzyme Activity vs Fatty Tail Length. Fatbergs are comprised of a range of fats - different fatty acid tail lengths can alter the degradation and solubility properties of fats within the fatberg. **A.** Rate at which Bacillus thuringiensis lipase hydrolyses fats based upon their chain length. The data has been adapted from "Identification of lipolytic enzymes isolated from bacteria indigenous to Eucalyptus wood species for application in the pulping industry." (https://2019.igem.org/File:T--Warwick--2019-Fat-Chain-Vs-Lipase-Archive.jpg) Bacillus thuringiensis was selected as it is closest to the Bacillus Subtilis Lipase that has been characterised by the iGEM team.
B. Integration of lipolysis rate into the biochemical *in vivo* model.

The many variants of fats within the model express different reaction rates with the lipase enzyme. A Bacillus thuringiensis lipase in **Figure 4A** to identify individual reaction rates for the fats. The effect of unsaturation on enzyme rate was considered, although the lack of literature resulted in a coefficient of 70% to be selected for every double bond which the fatty acids expressed (derived from: www.ncbi.nlm.nih.gov/pubmed/16856313). The fatty acids with the same number Carbon number were selected as the base number, and the efficiency was reduced to 70% of the base number for every desaturated carbon double bond. For example, Palmitoleic acid tail is 16 carbons long and has one desaturated carbon double bond. The relative efficiency was the same as Palmitate (as both tails have 16 carbon atoms). Where Palmitate had 50U/ml of Enzyme Activity, the relative rate for our model is double the Enzyme Activity (meaning 100% relative activity for the example). The original enzyme rate (Km) of 0.256 is increased by 50% to simulate the efficiency increase in digestion between a pNP molecule and the native Glycerol molecule which the active site would have evolved to target (Km now 0.384). As a double bond exists within Palmitoleic tail, the final calculation is "Enzyme Activity * Saturation Coefficient * New Km" (100%* 70% * 0.384): the final Palmitoleic fat Km is 0.2688 mmol/ml, which is shown implemented in **Figure 4B.**

The many variants of fatty acids within the model also express different solubilities in water, which can be found through the Pubchem (pubchem.ncbi.nlm.nih.gov/) entries on their respective fatty acid: **{Fatty Acid, Solubility in mg/L at 25°C};** {Oleic-Acid, 0.0115 mg/L at 25 °C}; {Palmitic-Acid, 0.04 mg/L at 25 °C}; {Palmitoleic-Acid, 0.447 mg/L}; {Stearic-Acid, 0.597 mg/L at 25 °C}; {Linoleic-Acid, 1.59 mg/L at 25 °C}; {Mristic-Acid, 22 mg/L at 30 °C}. *Mristic-Acid did not have an entry at 25°C and so was substituted with 30°C solubility.* The wash rate equation was then defined as “Fatty-Acid -> ((25-Wash-Coeffiient)/25) * Fatty-Acid” (for example Linoleic acid was defined as (25-1.59mg/L)/25 = 0.9364 where the wash rate equation is “Linoleic-Acid -> 0.9364 * Linoleic-Acid” and k1 was defined as 0.001). The wash rate simulates the rate at which the fatty acid product from the lipolysis of fats is removed by the flow of water in the sewer. Rates based upon initial concentration and reverse reaction were also used to simulate the flow of fats back into the fatberg.

The model can be found on the iGEM webiste:
2019.igem.org/File:T--Warwick--2019-COPASI-Model.zip

Results

General Trends ALL

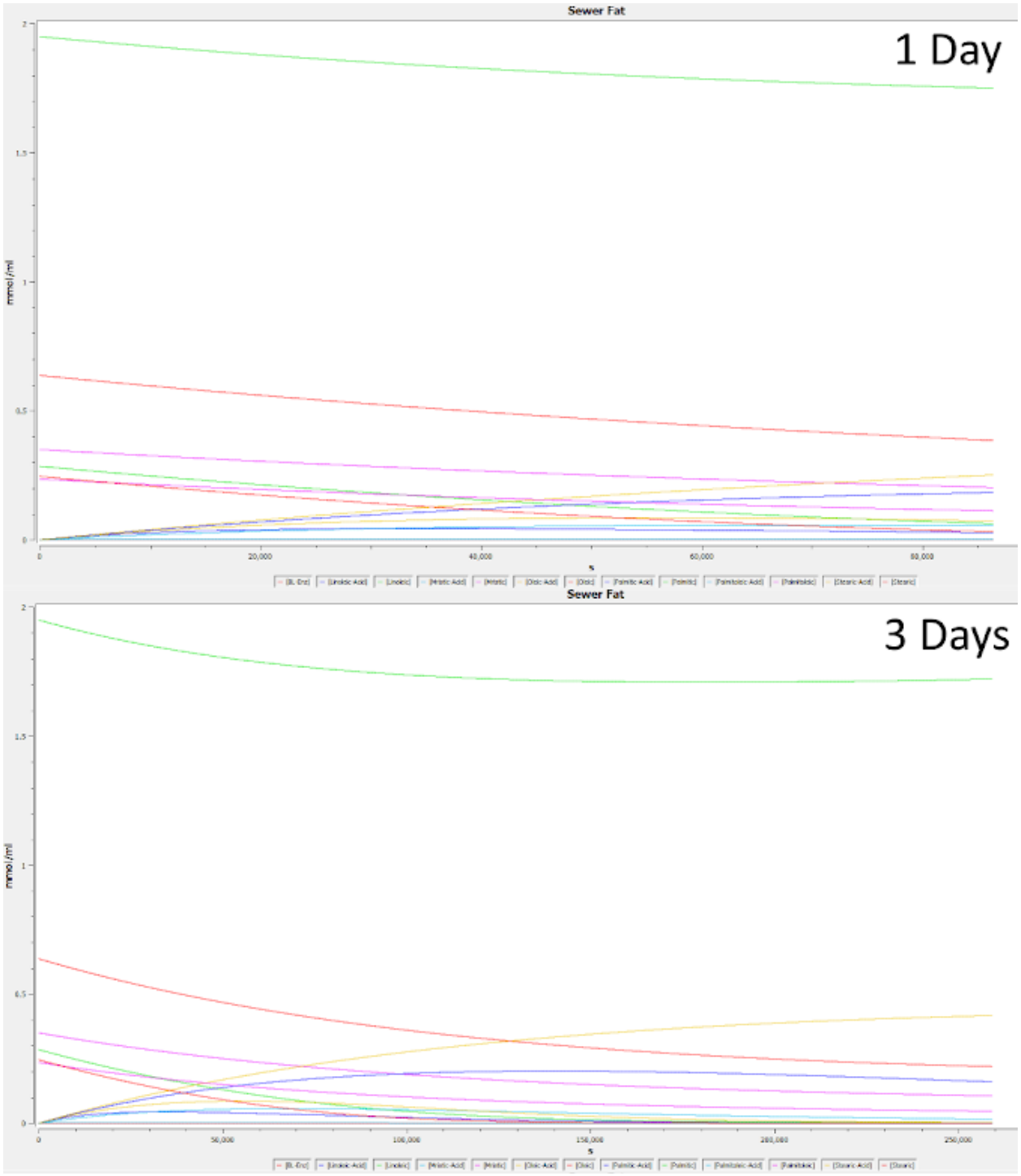

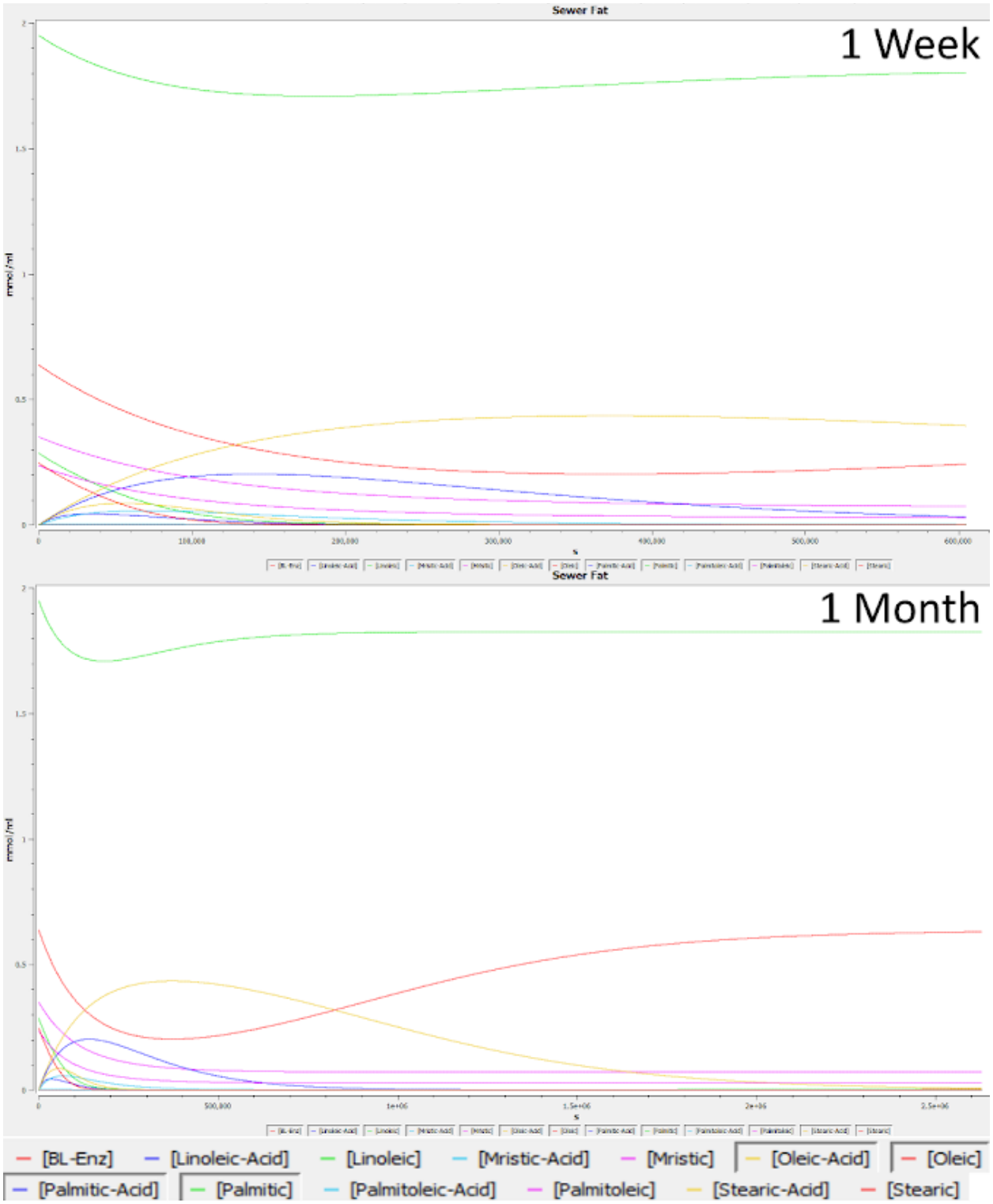

Figure 5. Effects of Extended Time on *In Vivo* Model Fatberg Behavior. The *in vivo* model was tested at *1 day, 3 days, 1 Week and 1 Month*. No parameters were altered, only the time window was increased.

Figure 5 visually describes how model time periods can alter perception of actual performance. As the time period over which the model is generated increases, the slower the rate at which fats degrade. Some fats begin to recover, and the model shows fatberg regeneration. On the first day, all fats show clear degradation and a strong trend to fatberg destruction; however when approaching the third day some of the fats with higher initial concentrations appear to plateau, avoiding destruction. By the first week two fats in particular (oleic and palmitic tails) begin to show recovery, and after an entire month the two fat concentrations in the fatberg have completely regenerated, showing that synthetic enzymes are only a temporary solution to fatberg formation. Constant enzyme application would have to be performed in order to destroy a fatberg.

Enzyme Concentration Trends

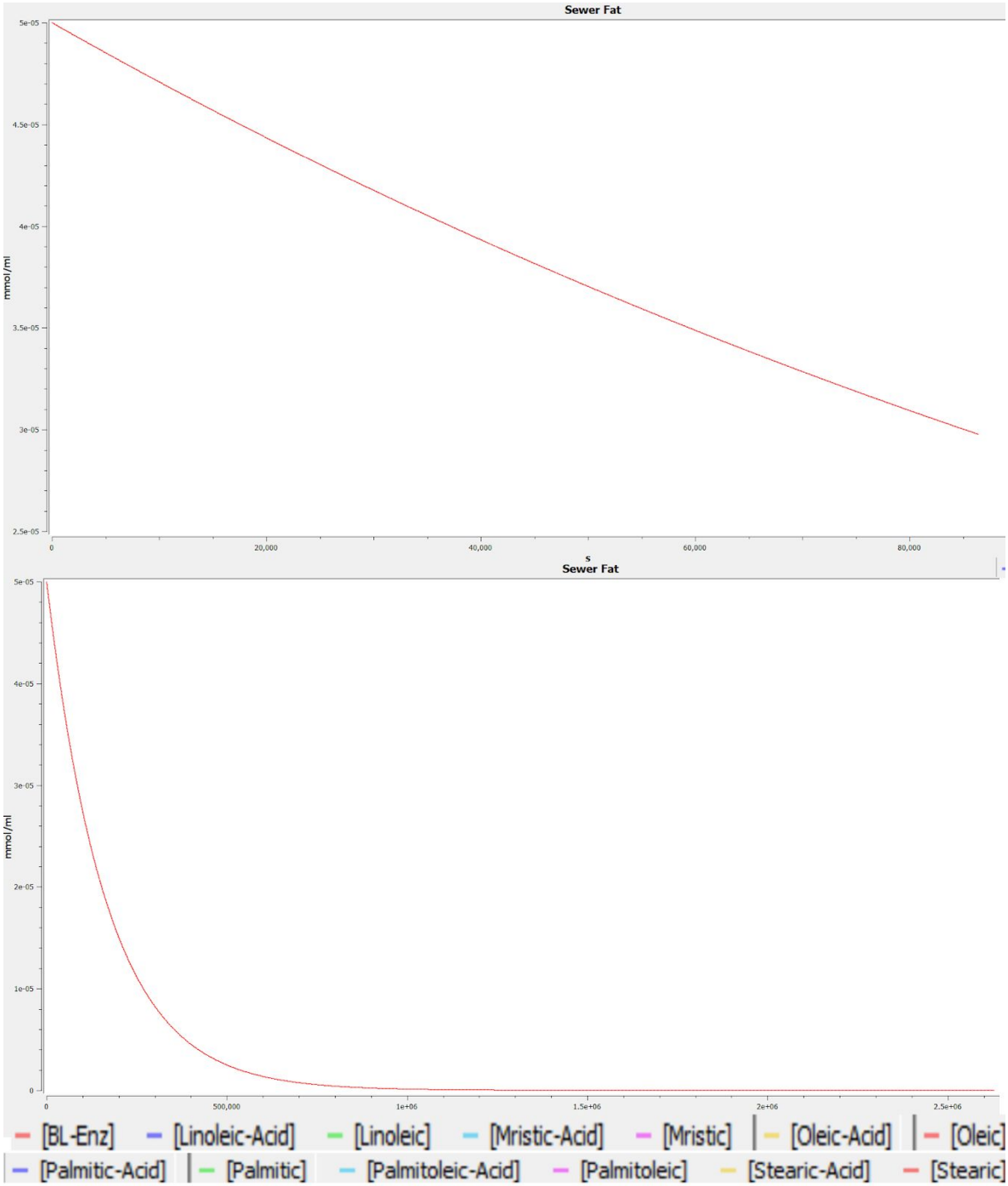

Figure 6. Lipase Enzyme Degradation in Fatbergs. The lipase enzyme degrades over time due to wash factors (being washed away) and denaturation. An initial observation of enzyme concentration over the course of a single day (top) demonstrates a sharp decline. The strength of decline is clear in the month model (bottom), where the enzyme concentration has diminished to near zero after only 12 days.

Palmitic and Oleic Fat Degradation

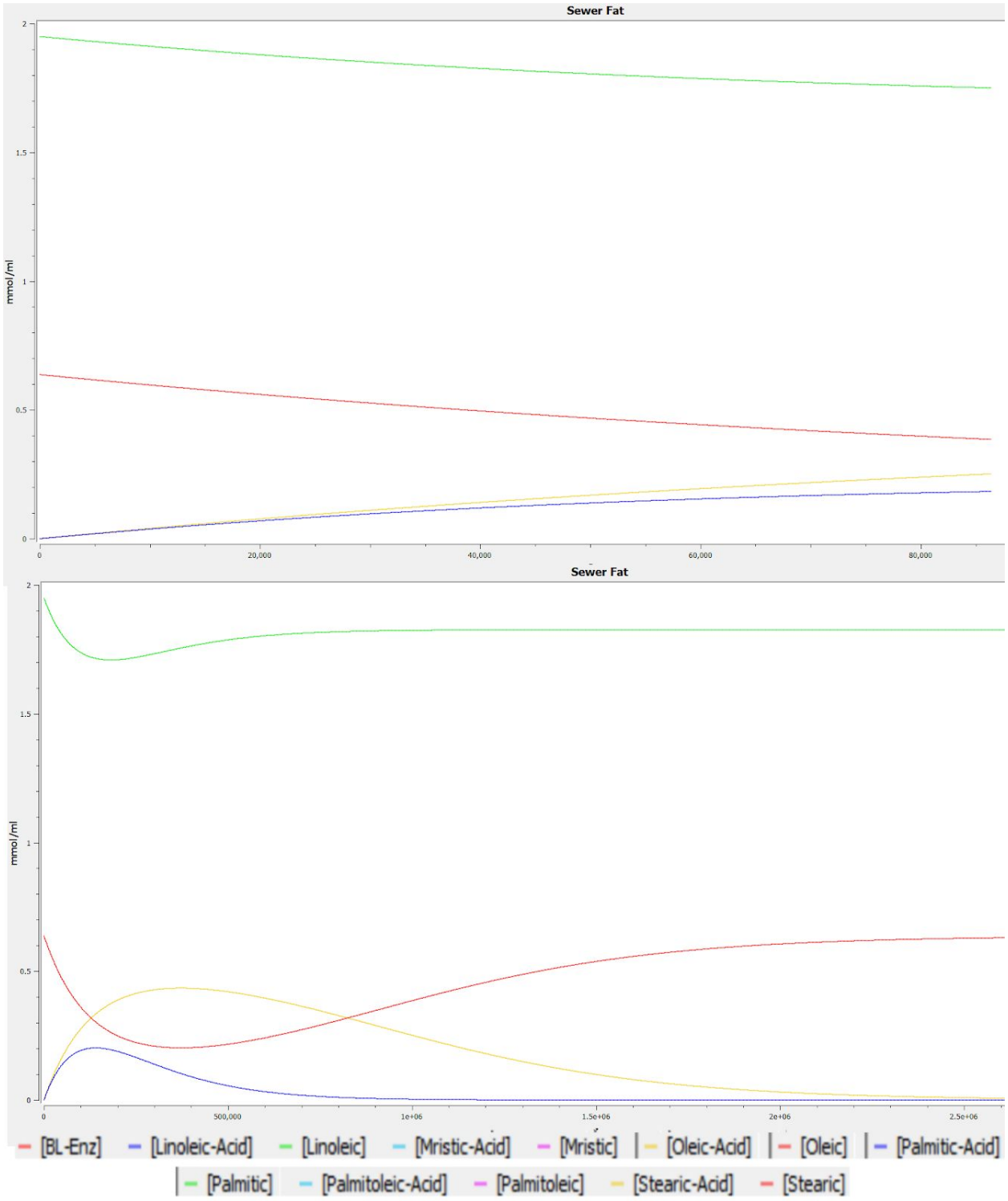

Figure 7. Palmitic and Oleic Fat Degradation. The graphs present Palmitic and Oleic fats being degraded (where red shows Oleic fat, green shows Palmitic fat, Yellow shows Oleic Acid and blue shows Palmitic Acid). A fatty acid tail becomes more susceptible to solution and wash factor after lipolysis from the fat.

Both Palmitic and Oleic fat comprise the majority of the fatberg. After lipase action a fatty acid tail becomes more susceptible to solution and wash factor after lipolysis from the fat, which is demonstrated in Figure 7 by the sharp decline of the Oleic acid and Palmitic acid. Both Palmitic and Oleic fats regenerate over the course of the month, unlike the other fats, and compose the majority of the fatberg. Further investigation into unique properties of the fats reveal that they also express the lowest solubilities by several fold over any other fats. The complex biochemical model demonstrates an otherwise overlooked connection between fatberg composition and fatberg solubility. Palmitic and Oleic fats are highly expressed in fatbergs, not only due to being highly common, but also due to their extremely poor solubility relative to other fats.

Figure 5 and **Figure 7** define a clear problem in synthetic biological solutions to fatbergs. The current approaches to fatberg destruction are temporary, and fatbergs will regenerate without preventative measures. In order to most effectively target fatbergs, a public outreach campaign is essential. Warwick iGEM 2019 have approached fatbergs through an educational public engagement campaign as the current biological approaches are futile in the long-term without public support.

Limitations

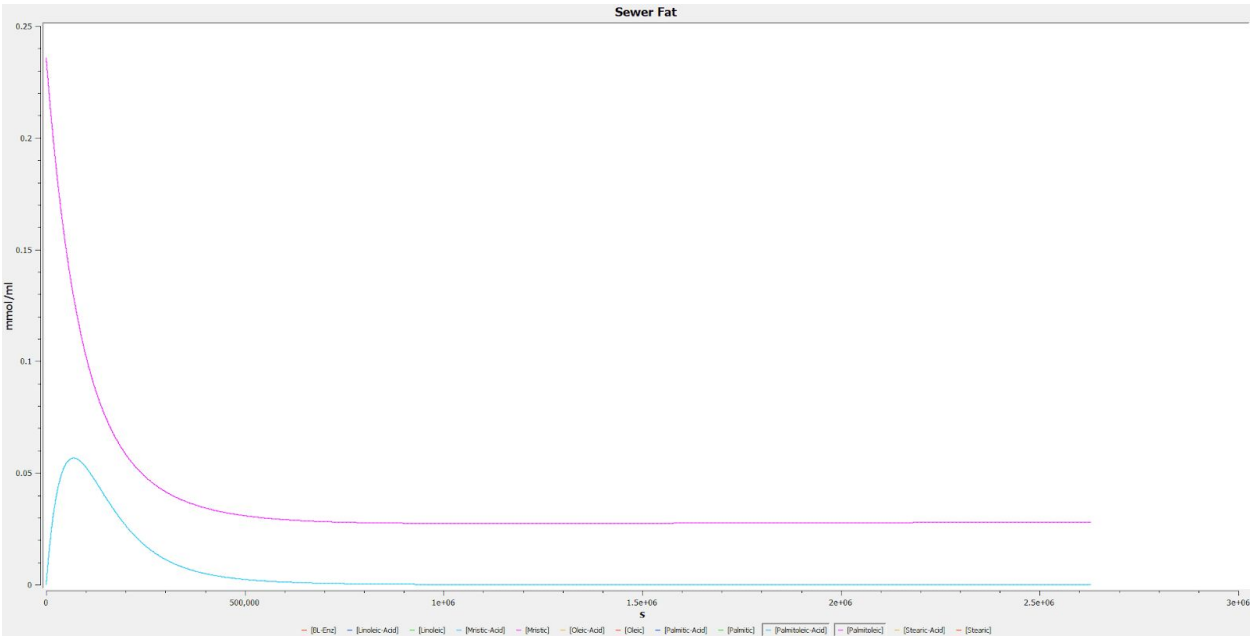

Figure 8. Palmitoleic Acid - Limitation Example. Palmitoleic Fat (purple) and Palmitoleic acid (light blue) demonstrate a limitation in the model. Simulations for long periods of time show degradation of Palmitoleic fat below the regeneration capacity, where the fatberg is essentially depleted.

In order to justify conclusions from the biochemical model, the limitations of the results must be considered and which assumptions may be inappropriate. **Figure 8** demonstrates a limitation of the model, where a fat of a specific type may be degraded beyond the regeneration threshold for itself, whilst the fatberg is still present. Each fat seems to express an individual regeneration capacity rather than one linked to the entire fatberg. Currently the phenomena causes fatbergs to become almost completely composed of Oleic and Palmitic fats after a month beyond enzyme treatment. The conclusion is not valid, as the effect is caused by an error in the behavior of the model rather than an effective simulation of real properties.

Fatty acids dissolve poorly in water, and the wash factor may show greater strength in the model than in the real environment. The model may be limited in showing fatty acid escape from fatberg, in reality the fatty acid wash factor may be so low that it becomes negligible, meaning fatty acids never escape from the fatberg, and the fatberg mass does not decrease at a sufficient rate to reach destruction, even ignoring enzyme degradation rate.

The model also does not consider enzyme solubility in water, and lack of enzyme solubility in hydrophobic environments (such as the fatberg itself). The model presents interactions between chemicals as if the entire environments are exposed to one another, wherein reality the hydrophobic (fats and fatty acids) and water soluble (enzymes) environment will interact poorly.

To conclude, in spite of some of the limitations presented within the model, insight into fat behavior can be derived - the biochemical model demonstrates why public engagement and outreach campaigns are currently critical to fighting the fatberg problem. The warwick iGEM 2019 team further explore the public engagement campaigns and fatberg problems on their wiki:
https://2019.igem.org/Team:Warwick/Human_Practices
https://2019.igem.org/Team:Warwick/Public_Engagement